RSC Advances

ROYAL SOCIETY OF CHEMISTRY

www.rsc.org/advances

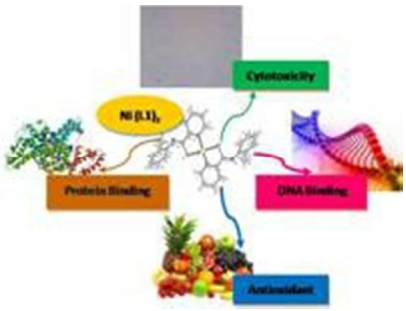

Graphical Abstract
34x25mm (150 x 150 DPI)

RSC Advances

RSC Publishing

ARTICLE

Synthesis and Structure of Nickel(II) thiocarboxamide Complexes: Effect of ligand substitutions on DNA/Protein binding, Antioxidant and Cytotoxicity

Cite this: DOI: 10.1039/xoxxoooooox

Received ooth January 2012,
Accepted ooth January 2012

DOI: 10.1039/xoxxoooooox

www.rsc.org/

Ramasamy Raj Kumar, Mohamed Kasim Mohamed Subarkhan, Rengan Ramesh*

Four low spin d8 nickel(II) square planar complexes with general formula [Ni(L)2] (where L=Monobasic N, S bidentate thiocarboxamides) have been synthesized from the reaction of Ni(OAc)2·4H2O with 2 equivalent of thiocarboxamide ligands in ethanol. The complexes have been fully characterized by analytical, spectral (FT-IR, UV-Vis, 1H and 13C NMR) and single crystal X-ray methods. Molecular structure of one of the complexes indicates a mono anionic bidendate coordination of thiocarboxamide ligands to the nickel via pyridine nitrogen and thiolate sulphur and reveal a square planar geometry. The binding interaction of nickel(II) thiocarboxamide complexes with calf-thymus DNA (CT-DNA) was studied by electronic and emission spectroscopic methods revealed that complexes 1-4 could interact with CT-DNA via intercalation mode. DNA cleavage experiment shows that all the complexes cleave pUC19 supercoiled DNA in the presence of an activator like H2O2. The CD spectral study shows that binding of the complexes to DNA does not lead to any significant changes in the conformation of CT-DNA. Further, the protein binding ability of the nickel(II) thiocarboxamide complexes with the BSA was investigated by UV-Vis, fluorescence and synchronous fluorescence methods and a static quenching mechanism was observed for their interaction with BSA. The free radical scavenging ability of all the complexes was evaluated by in vitro antioxidant assays involving DPPH radical, hydroxyl radical and nitric oxide radical and was found to be excellent. Moreover, the efficiency of complexes 1-4 to arrest the growth of HeLa and MG 63 cell lines has been studied along with the cell viability test against the non-cancerous cells NIH-3T3 under in vitro condition. Complex 3 was found to be the highest anticancer activity among the nickel complexes.

*School of Chemistry Bharathidasan University,
Tiruchirappalli – 620 024, Tamil Nadu, India.
Corresponding author:
E-mail: ramesh_bdu@gmail.com;
Fax: +0091-431-2407045/2407020; Tel: +91-431-2407053

†Electronic Supplementary Information (ESI) available:
[The ^{1}H, ^{13}C NMR and UV-Vis spectra of the complexes (1-4).
MTT assay of the complex 3. CCDC reference number 1033617.
See DOI: 10.1039/b000000x/

Introduction

The interaction of transition metal complexes with DNA has been studied with the aim of developing probes for nucleic acid structures and chemotherapy agents.[1] Numerous biological experiments have been demonstrated that DNA is the primary intracellular target of anticancer drugs; DNA can cause damage in cancer cells, blocking the division and resulting in cell death.[2] Cisplatin and its analogues are still one of the world best-selling anticancer drugs. The limitation of using cisplatin leads to side effects and dose-limiting nephrotoxicity and the development of drug resistance prevents its potential efficacy.[3] There is considerable attention focused on the design of new metal-based anti cancer drugs that exhibit enhanced selectivity and novel modes of DNA interaction like non-covalent interactions that mimic the mode of interaction of

biomolecules.[4] Among the anticancer drugs, ruthenium(III) analogues such as indazolium trans- [tetrachlorobis(1H-indazolone ruthenate III)] NAMI and (trans-tetrachlorobis(indazole)ruthenate(III)KP 1019 complexes show promising anticancer activity.[5] Though several examples of DNA-targeted metal complexes of platinum, ruthenium, cobalt and copper are known in the literature,[6-9] studies on nickel complexes are relatively less.

BSA is a soluble protein and it facilitates the many physiological functions such as maintain osmotic pressure, p^H of blood, metal ions, steroids and drugs in blood stream. Knowledge of interaction mechanisms between drugs and plasma proteins is very important to understand the pharmacokinetics and pharmacodynamics of a drug. Drug binding influences their absorption, distribution, metabolism, excretion, and interaction with the target tissues.[10] Bovine serum albumin has proven to have a high homology and a similarity to human serum albumin in conformation and sequence.[11] Antioxidants are the compounds which prevent it from ageing and various disease associated with oxidative damage inside the human body system.[12, 13] Free radicals including reactive oxygen species (ROS) which is generated from metabolism and or by the environmental factors interact directly to the biological systems and the unbelievable generation of free radicals have been implicated with variety of chronic diseases including cancer, diabetes, arthritis, neurodegenerative disorders and atherosclerosis [14, 15].

Researchers have become increasingly interested in the coordination chemistry of nickel complexes as models for the active sites in nickel containing enzymes.[16, 17] The report on the role of nickel in bioinorganic chemistry has been rapidly expanding. Nickel(II) complexes with nitrogen and sulphur donor ligands are also highly interesting[18] because several hydrogenase[19] and carbon monoxide dehydrogenase[20] contain such nickel complexes as their active site. The effect of structure and composition of nickel(II) complexes with salicylidene schiff base ligands on their DNA/protein interaction and cytotoxicity has been reported.[21] Synthesis, structure, DNA and protein binding studies, and cytotoxic activity of nickel(II) complexes containing 3,3-dialkyl/aryl-1-(2,4-dichlorobenzoyl)thiourea ligands have been described.[22] The biological evaluation of substituted salicaldehyde thiosemicarbazone with new nickel(II) complexes towards the synthesis, DNA/protein binding and mitochondrial mediated apoptosis in human lungcancer cells (A549) via ROS hypergeneration and depletion of cellularantioxidant pool has been reported recently.[23]

Like Schiff bases, thioamides are excellent chelating ligands and are the sulphur analogues of amides. The first thioamides was synthesiszed in 1815; considerable effort has been directed towards the synthesis and characterization of the metal complexes of aromatic thioamides in recent years.[24] Thiocarboxamide derivatives and their metal complexes have raised interest because of their well known chelating ability and structural flexibility which leads to high pharmacological properties. Though some nickel complexes containing various ligands are known for their biological properties, nickel(II) complexes bearing thiocarboxamide are not reported. Hence, we wish to describe here the synthesis and characterization of a new series of nickel(II) thiocarboxamide complexes. The pharmacological properties of the nickel(II) thiocarboxamide complexes for DNA/Protein binding interactions, DNA cleavage, free radical scavenging activity and cytotoxicity were explored. Further, the substituent effect of thiocarboxamide ligand upon the biological properties was also studied.

Results and Discussion

The treatment of $(CH_3COO)_2Ni{\cdot}4H_2O$ with 2 equivalent of the ligand in ethanol medium under reflux for 5h resulted in the formation of new square plannar nickel(II) thiocarboxamide complexes of the formula $[Ni(L)_2]$ (Scheme1). In this reaction the acetate anion acts as the base and facilitates the formation of these complexes. All the complexes are stable in air, light, colour and soluble in organic solvents like $CHCl_3$, DMF and DMSO respectively. The analytical and spectral data (FT-IR, UV-Vis and NMR) confirmed the stiochiometry of the complexes.

The important IR bands of the complexes 1-4 in a KBr pellet showed the useful information about the coordination mode of the ligands and the molecular structure of the complexes. In principle, the ligand thiocarboxamide exhibit thione-thiol tautomerism, since it contains a thioamide –NH-C=S functional groups. The FT-IR spectra of the free ligands show a medium to strong band in the region 3310-3214 cm^{-1} which is characteristic of the N-H functional group. The free ligands also display $\gamma_{C=S}$ absorptions in the region 820-898 cm^{-1}.The bands due to γ_{N-H} and $\gamma_{C=S}$ stretching vibrations are not observed in the complexes suggesting that the ligands undergo tautomerization and subsequent coordination of the thiolate form during complexation.[25]

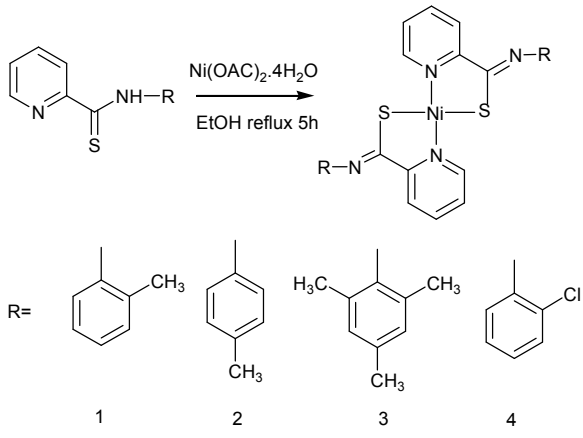

Scheme 1: Synthesis of nickel(II) thiocarboxamide complexes.

The IR spectra of the complexes did not display γ_{S-H} at 2589-2572 cm^{-1} indicating the deportation of the thiol proton prior coordination. This supports the lengthening of the C-S

bond that is observed in the molecular structure. Further, new bands appeared around 1612-1634 and 1202-1254 cm^{-1} which corresponds to $\gamma_{C=N}$ and γ_{C-S} of the thiocarboxamide complexes. A week intensity band is observed at 1098-1081 cm^{-1} characteristic of the coordinated pyridine nitrogen to metal.[26]

The absorption spectra of all the nickel(II) thiocarboxamide complexes 1-4 was recorded in chloroform solution in the range 200-800 nm at room temperature and all the complexes showed four bands with absorption maxima in the region 237–472 nm and shown in Fig. S9-S12 (ESI†). In the visible region, for square planar complexes of nickel(II), three spin allowed singlet-singlet d-d transitions from $^1A_{1g}$ to $^1A_{2g}$, $^1B_{1g}$ and ^1E_g are expected. The high intensity bands in the region of 237-270 nm region corresponds to ligand-centered (LC) transitions and have been designated as π–π* and n–π* transitions for the electrons localized on the thiocarboxamide ligand. The medium intensity band in the region 340-350 nm is due to Ligand-Metal Charge transfer processes. The longer wavelength band in the region of 466-472 nm corresponds to the d-d transitions of a d^8 low-spin Ni^{II} in slightly distorted square-plannar geometry. The pattern of the electronic absorption spectra of all the complexes indicate the presence of a square planar environment around nickel(II) ion, similar to that of other mononuclear square planar nickel(II) complexes.[27]

The ^1H NMR and ^{13}C NMR spectra of complexes 1-4 were recorded in $CDCl_3$ and are shown in Fig.S1-S8 (ESI†). The ^1H NMR spectra of complexes 1-4 indicate that the coordination of the nickel atom to the pyridyl nitrogen, causes a significant downfield shift for the proton adjacent to the nitrogen (H-1), in the range of δ8.2 ppm in all the complexes. This arises from an σ effect based on electron donation to nickel(II) via the nitrogen lone pair, and confirms the coordination mode of the nickel ion to the pyridine nitrogen. The aromatic protons and methyl protons are observed in all the complexes in the region of δ6.9-8.2 ppm and δ 2.1-2.3 ppm respectively. A sharp singlet that appeared for the –NH protons of the free ligand in the region δ11.9-11.3 ppm are absent in all the complexes supporting the thione-thiol tautomerisation and coordination of the thiolate sulphur to the nickel(II) ion.[28] In ^{13}C NMR spectra the signal corresponds to the thioketone carbon, which moves upfield from δ 190-180 ppm in the ligand to δ167-170 ppm in the nickel(II) complexes, and thus a reduced C-S bond order on coordination is observed.

Description of the solid state structure

The solid state X-ray molecular structure of one of the nickel(II) complexes, viz., $[Ni(L)_1]$ (1) has been determined by single crystal X-ray diffraction study to predict the coordination mode of thiocarboxamide ligands to the nickel and stereochemistry of the complexes. The ORTEP view of complex 1 is shown in Fig.1. The summary of data collection and refinement parameters are given in Table 1 whereas selected bond lengths and bond angles are presented in Table 2. The complex crystallizes in the "P21/c" space group. The nickel ion is tetra co-ordinated in a square planar geometry by two ligand molecules acting as monoanionic bidendate N, S-donor via pyridine nitrogen and thiolate sulphur. The ligand is trans position with respect to the C-N bond and the complex is centrosymmetric around the nickel center. Nickel is therefore sitting in a N2S2 coordination environment, which is square plannar in nature as reflected in all the bond parameters around nickel. In the complex thiocarboxamide ligand binds with metal center at N and S forming two five membered chelate ring with bite angle N(1)–Ni(1)-N(1) 92.54(4)° and S(1)-Ni(1)-N(1) 87.46(4)°. The bond lengths of Ni(1)–N(1) and Ni(1)–S(1) are 1.941(1) and 2.1807(5) Å respectively. The bond distances and bond angles are in good agreement with reported data on related nickel(II) complexes with square plannar geometry.[29] As all the four nickel(II) complexes display similar spectral properties, the other three complexes are considered to have similar structures as that of complex 1. The X-ray determination confirms the structure proposed on the basis of spectroscopic data, consistent with metal bivalency and the mono ionised nature of the ligand in complexes.

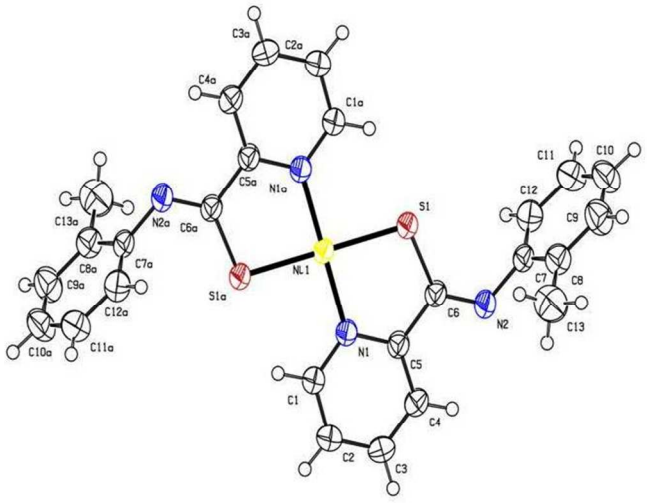

Fig: 1 The ORTEP diagram of the complex-1 at 50% probability level

DNA binding properties - Absorption Spectral Studies

UV-visible spectroscopy is a simple and reliable method to determine the binding affinity of metal complexes with DNA. In general, hyperchromism and hypochromism are the spectral features of DNA concerning the changes of its double helix structure. Additionally, the existence of a red shift is indicative of the stabilization of the DNA duplex.[30] The interaction of the complexes with CT-DNA was followed by recording the UV-visible spectra of the system. The experiment was carried out keeping the concentration of the nickel(II) thiocarboxamide complexes (1μM) as constant and varying the concentration of the CT-DNA (0-50μM). The absorptions bands at 273 nm and 321 nm in the complexes were considered for the corresponding adsorptivity changes upon the incremental addition of CT-DNA.

Table 1: Crystal data and structure refinementof the complex **1**.

Empirical formula	$C_{26}H_{22}N_4S_2Ni$
Formula weight	513.29
Temperature (K)	296(2)
Radiation type	Mo Kα
Wavelength (Å)	0.71073
Crystal system	Monoclinic
Space group	$P2_1/c$
a (Å)	6.5753(4)
b (Å)	9.3025(6)
c (Å)	19.5943(12)
α (°)	90.00
β (°)	96.416(6)
γ (°)	90.00
Volume (Å3)	1191.03(13)
Z	2
Dcalcd. (Mg m–3)	1.431
μ (mm–1)	1.012
F(000)	532
Crystal size (mm)	0.54×0.21×0.18
Theta range (°)	2.09-29.96
Limiting indices	-9 ≤h≤9, -13≤ k ≤ 10, –27 ≤ l ≤ 25
Reflections collected/unique	12482/3439
Refinement method	Full–matrix least–squares on F2
Data/restraints/parameters	3439/0/152
Goodness–of–fit	1.104
Final R indices [I>2σ(I)]	R1 = 0.0322, wR2 = 0.0970
R indices (all data)	R1 = 0.0430, wR2 = 0.1012
Largest diff. peak and hole	0.47 and -0.46 e. A^{-3}

Table 2: Selected bond lengths (Å) and bond angles (°) of the complex-**1**

Complex	1
Ni (1) –N (1)	1.941(1)
Ni (1) –S (1)	2.1807(5)
S (1) – C (6)	1.725(1)
N (1) – C (1)	1.345(2)
N (1) – C (5)	1.356(2)
N (2) – C (7)	1.421(2)
N (2) – C (6)	1.271(2)
S (1) – Ni (1)-S (1)	180.00 (2)
S (1) – Ni (1)-N (1)	92.54 (4)
N (1) – Ni (1)-N (1)	180.00 (5)
Ni (1) - S (1)-C (6)	100.28 (5)
Ni (1)-N (1) -C (1)	123.7 (1)
Ni (1)-N (1)-C (5)	119.7 (1)
C (1)-N (1) -C (5)	116.6 (1)
C (6)-N (2) -C (7)	121.2(2)
N (1) – C (1)-H (1)	118.2 (2)
N (1) – C (1)-C (2)	123.7 (2)
N (1) – C (5)-C (4)	122.3 (1)
N (1) – C (5)-C (6)	116.8 (1)
S (1) – C (6)-N (2)	126.6 (1)
S (1) – C (6)-N (5)	115.3 (1)
N (2) – C (6)-C (5)	118.0 (1)
N (2) – C (7)-C (8)	117.8 (2)
N (2) – C (7)-C (12)	121.5 (2)
H (1) – C (1)-C (2)	118.1 (2)

The electronic absorption spectra of the complexes **1-4** without as well as the added CT DNA are shown in Fig.2. The addition of CT-DNA to the complexes showed only hypochromism of about 29.40%, 28.29%, 17.85% and 27.45% with 3, 2, 2 and 2 nm of bathochromic shift of complexes (1-4) suggesting that the nickel(II) thiocarboxamide complexes bind strongly to CT-DNA via the intercalative mode. The observed hypochromism is due to stacking interaction between the aromatic chromophores of the complexes and DNA base pairs consistent with the intercalative mode of binding. These observations are similar to those reported earlier for various metallointercalators.[31]

In order to determine relative binding strength of complexes with CT-DNA, intrinsic binding constants were obtained by monitoring the changes in both the wavelength as well as corresponding intensity of absorption of the high energy bands of complexes 1-4 upon increasing the concentration of added DNA. The intrinsic binding constants have been determined from the equation(1):[32]

$$[DNA]/ [\varepsilon_a-\varepsilon_f] = [DNA]/ [\varepsilon_b-\varepsilon_f] +1/K_b [\varepsilon_b-\varepsilon_f] \quad (1)$$

Where, [DNA] is the concentration of DNA in base pairs, ε_a is the extinction coefficient of the complex at a given DNA concentration, ε_f is the extinction coefficient of the complex in free solution and ε_b is the extinction coefficient of the complex when fully bound to DNA. A plot of $[DNA]/[\varepsilon_b-\varepsilon_f]$ versus [DNA] gave a slope and intercept equal to $1/[\varepsilon_b-\varepsilon_f]$ and $(1/K_b)$ $[\varepsilon_b-\varepsilon_f]$, respectively. K_b was calculated from the ratio of the slope to the intercept.

The intrinsic binding constant (K_b) values have been found to be $1.14(\pm0.05)\times10^5M^{-1}$, $0.98(\pm0.10)\times10^5M^{-1}$, $0.97(\pm0.08)\times10^5M^{-1}$ and $0.89(\pm0.06)\times10^5M^{-1}$corresponding to the complexes **1-4** respectively. From this experimental result, it very clearly shows that the increase in electron donating ability of the substituent at the terminal nitrogen of the ligands increases the DNA binding ability of the complexes. The presence of trimethyl groups on the phenyl ring in the complex 3 hindered the intercalation and hence resulted in lower binding constant value. The presence of electron withdrawing (chlorine) group in complex 4 has almost lower binding constant value is due to decrease in the electron density on the metal centers. Further the DNA binding ability increases when the electron donating ability of the substituent at terminal nitrogen of the thiocarboxamide ligands. From the electronic absorption titration studies all the complexes interact with DNA via intercalative mode and complex **1** binds to CT-DNA more strongly than the other complexes. Although, results of the absorption spectral studies shows that the complexes bind to DNA via intercalation, the actual binding mode needs to be proved by some experiments.

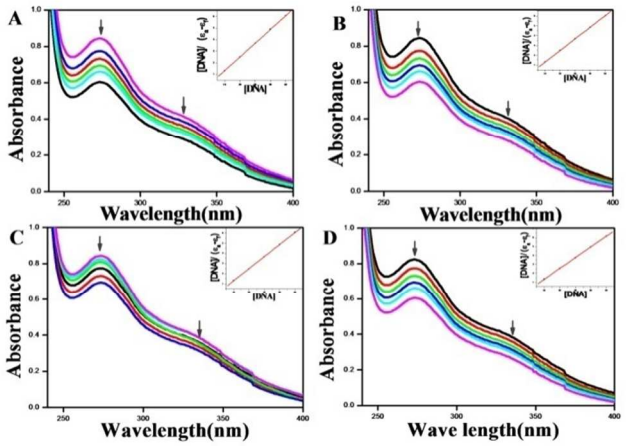

Fig: 2 The Absorbance quenching curves of complex bound to DNA 1(A), 2(B), 3(c) and 4(D)[DNA]= 0-50 µM,[Complex]= 1 µM (Inset: plot of [DNA/εa-εb]/[DNA]).

Luminescence titration in the presence of Ethidium bromide

Further, the fluorescence spectral titrations were also performed to study the competitive DNA binding of complexes by monitoring changes in the emission intensity of ethidium bromide (EtBr) bound to CT-DNA by adding the complexes as quenchers. As the nickel(II) thiocarboxamide complexes is not fluorescence we have done competitive emission experiments using ethidium bromide as an optical probe. EtBr is a plannar cationic dye can intercalate non-specifically into DNA and it can form soluble complexes with nucleic acids which causes it to fluoresce strongly. The emission intensity of EtBr in buffer medium is enhanced due to its stacking interaction of the plannar phenanthridinium ring between the adjacent DNA base pairs, eventhough it is quenched by the solvent molecules and the fluorescence intensity is highly enhanced upon the addition of CT-DNA. When complex was added to DNA pretreated with EtBr, the emission intensity was decreased due to competition by the complex for the EtBr intercalating sites. The emission spectra of EB bound to CT-DNA in the absence and presence of compounds have been done for [EB] =10µM and [DNA]= 10µM upon the incremental addition of nickel(II) thiocarboxamide complexes [0-60µM]. The changes were observed in the fluorescence spectra of EtBr on its binding to CT-DNA are used for the interaction study between the DNA and metal complexes. The quenching constant has been calculated from the Stern-Volmer equation (2):

$$I_0/I = K_q [Q] + 1 \quad (2)$$

Where $I_0$is the emission intensity of the absence of quencher, I is the emission intensity of the presence of quencher, K_q is the quenching constant, [Q] is the quencher concentration. K_q is the slope obtained from the plot of I_0/I versus [Q] (shown as insets in Fig.3).The quenching plots illustrate that the quenching of EtBr bound to CT-DNA by the nickel(II) thiocarboxamide complexes are in good agreement with the linear Stern-Volmer equation. The K_q values are obtained from the experiments are $1.13(\pm0.04)\times10^5M^{-1}$, $1.02(\pm0.12)\times10^5M^{-1}$, $1.01\times(\pm0.18)\times10^5M^{-1}$ and $1.00(\pm0.28)\times10^5M^{-1}$ respectively. Further the apparent DNA binding constant (K_{app}) were calculated from the following equation (3):

$$K_{EtBr}[EtBr] = K_{app}[complex] \quad (3)$$

(where the complex concentration has the value at a 50% reduction of the fluorescence intensity of EtBr, $K_{EtBr} = 1.0\times10^7$ M^{-1} and [EtBr] =10µM) were found to be $6.23\times10^5M^{-1}$, $5.81\times10^5M^{-1}$, $5.40\times10^5M^{-1}$, and $5.33\times10^5M^{-1}$ for complexes **1-4** respectively. The fluorescence quenching spectra of DNA-bound EtBr by complexes **1-4** shown (Fig.3) illustrate that, as the concentration of the complexes increases, the emission band at 605 nm(545 nm excitation)exhibited hypochromism up to 27.17%, 30.02%, 20.26% and 21.88% with hypsochromic shift of 2,1,2 and 1 nm of the initial fluorescence intensity for 1-4 respectively. The observed decrease in the fluorescence intensity clearly indicates that the EtBr molecules are displaced from their DNA binding sites and are replaced by the complexes under investigation.[33] Since these changes indicate only one kind of quenching process, it may be concluded that all of the complexes bind to CT-DNA via the same mode. On the basis of all the spectroscopic studies, we concluded that the nickel(II) complexes can bind to CT-DNA in an intercalative mode and the complex **1** binds to CT-DNA more strongly than the other complexes.

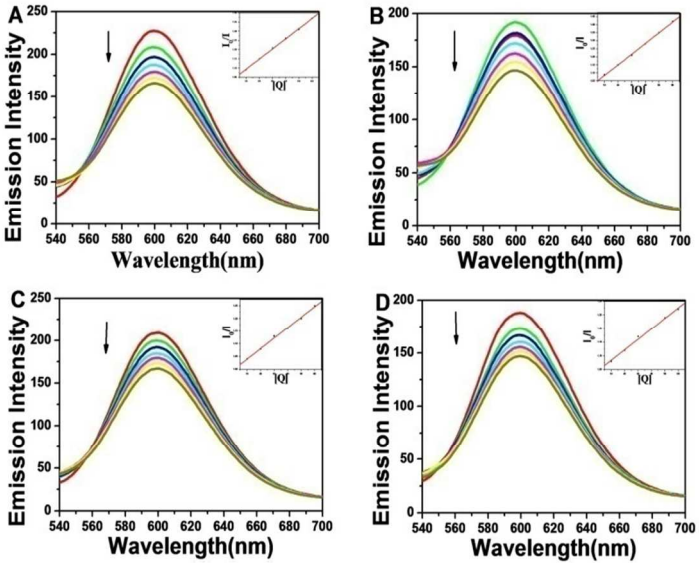

Fig: 3 The Fluoresence quenching curves of EtBr bound to DNA: **1**(A), **2**(B), **3**(c) and **4**(D), [DNA]= 10 µM ,[EB]= 10 µM, [Complex]= 0-60 µM (Inset: Plot of I_0/I Vs [Q]).

DNA cleavage

The DNA cleavage activity of all the complexes was explored by carrying out agarose gel electrophoresis experiments with plasmid pUC19 DNA (40μM in base pairs) and monitoring the conversion of supercoiled SC DNA (form-I) into nicked circular (form-II) in the presence of an activator like H_2O_2(60μM) in Tris-HCl buffer (p^H, 7.2) for 1h incubation at 37°C. The control experiments suggested that either untreated DNA or H_2O_2 does not show any cleavage (lane 1). From the experimental observations all the complexes cleave the pUC19DNA resulting in the conversion of form I (supercoiled form) in to form II (nicked circular) is shown in Fig. 4.The results suggested that the cleavage of the supercoiled form and formation of nicked circular form increased in the order **1>2>3>4**. It is believed that the more DNA cleavage ability of complex 1 is due to the reaction of metal ions with H_2O_2, which produces diffusible hydroxyl radicals or molecular oxygen and is expected to involve the Fenton-type chemistry.[34]

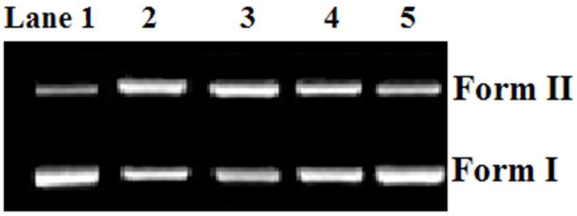

Fig: 4 Gel electrophoresis showing the DNA cleavage of the pUC19 DNA incubated at 37 ^{0}C 1h at a concentration of 35 μM of complex 1-4 in the presence of H_2O_2(60 μM) as a co-oxidant: lane 1: pUC19 DNA+ H_2O_2lane 2: pUC19 DNA+ H_2O_2+complex-1 lane 3: pUC19 DNA+H_2O_2+complex-2 lane 4: pUC19 DNA+ H_2O_2+complex-3 lane 5: pUC19 DNA+ H_2O_2+complex-4.

Circular dichromism

The CD spectrum is used to monitor the conformational changes of DNA when metal complex binds in solution. The circular dichronic spectrum of DNA shows a positive band at 275 nm (UV-Vis: λ_{max} 258nm) due to base stacking and negative band at 245 nm due to helicity of B- type DNA.[35] The simple groove binding and electrostatic interaction of the molecules show small or no perturbation on the base stacking and helicity, while intercalation increases the intensities of both the positive and negative bands. The CD spectrum of CT-DNA (60μM) in the presence of complex 1 at (20μM) is shown in Fig.5. From the experimental results, we observed the addition of the complexes to the DNA system increased the intensity of both the positive and negative bands of free DNA which is clear information of intercalation between the nickel(II) thiocarboxamide complexes and CT-DNA. The CD spectra indicates that the binding of complexes 1-4 to CT-DNA resulting to a significant increases in the intensities of the both positive and negative bands without any shift in peak positions which show that the binding of complexes does not lead to any significant change in the conformation of CT DNA.[36]

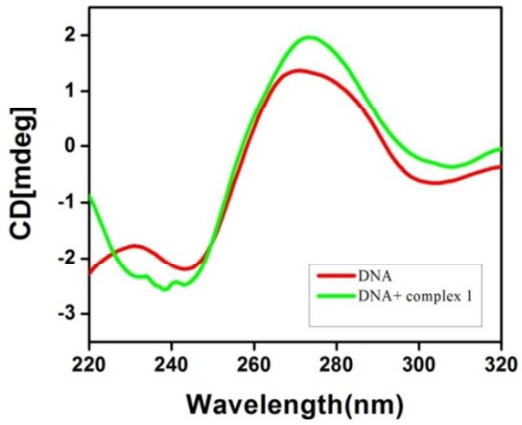

Fig: 5 Circular dichronic spectrum of CT-DNA (60μM) in the presence of complex-1 (20μM).

Viscosity study

Viscosity measurements are sensitive to changes in length of DNA, which are regarded as the least ambiguous and the most important tests of a DNA binding model in solution, providing strong evidence for the DNA binding mode of complexes. Lengthening of the DNA helix occurs on intercalation as base pairs are separated to accommodate the binding compound leading to an increase in DNA viscosity.[37, 38] The effects of the nickel(II) complexes on the viscosity of CT-DNA are shown in the (Figure 6). The values of $(\eta - \eta_o)^{1/3}$, where η and η_o are the relative viscosities of DNA in the presence and absence of the complex respectively, were plotted against [complex]/[DNA]. The viscosity of CT-DNA increased steadily with the increment of the nickel(II) complexes, similar to known intercalators[39] and the ability of the complexes to increase the viscosity of DNA follows the order 1>2>3>4. The results from the viscosity experiments confirm that the complexes intercalate into the DNA base pairs, as already established through absorption and fluorescence spectroscopic studies.

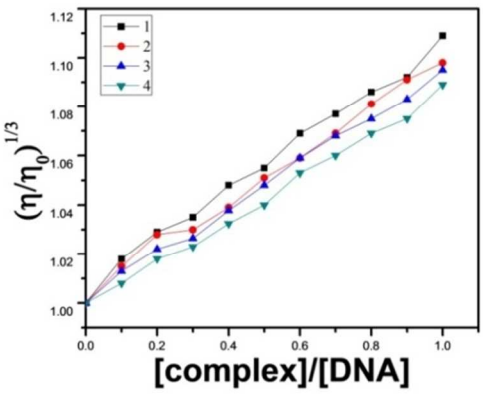

Fig: 6 Effects of increasing amount of complexes 1-4 on the relative viscosities of CT-DNA at 30.0±0 1 °C [DNA]= 5 μM and [complexes]=0-5 μM.

Protein binding studies

Fluorescence quenching measurements

Fluorescence quenching measurements have been widely used to study the interaction of metal complexes with proteins such as (BSA, HSA, lysozyme, etc.,).[40-42] The interaction of BSA with nickel(II) thiocarboxamide complexes was investigated by fluorescence measurement at room temperature by Stern-Volmer relation. A solution of BSA (1μM) was titrated with various concentrations of complexes (0-50 μM). Fluorescence spectra were recorded in the range of 300-400 nm upon excitation at 280 nm. The effects of complexes on the fluorescence emission spectrum of BSA are shown in Fig.7.The addition of the above complexes to the solution of BSA resulted in a significant decrease of the fluorescence intensity of BSA at 335 nm, up to 51.40, 59.27. 21.89 and 70.50%from the initial fluorescence intensity of BSA accompanied by a bathochromic shift of 3, 3, 3 and 4 nm for complexes 1-4 respectively. Addition of metal complexes to the solution of BSA resulted in the quenching of its fluorescence emission with red shift suggesting that the complex formed between the nickel(II) thiocarboxamide complexes and BSA is responsible for the quenching of BSA. The observed red shift is mainly due to the fact that the active site in the protein is buried in a hydrophobic environment. These results suggested a strong interaction of all the complexes with the BSA protein.[43, 44] The fluorescence quenching is described by stern-Volmer relation:[45]

$$I_0/I = K_{sv}[Q] + 1$$

Where $I_0$is the emission intensity of the absence of quencher, I is the emission intensity of the presence of quencher, K_{sv} is the Stern-Volmer quenching constant, [Q] is the quencher concentration. K_{sv} is the slope obtained from the plot of I_0/I versus [Q]. (Shown in Fig.8) was found to be $1.05(\pm0.24)\times10^6$ M^{-1}, $1.07(\pm0.12)\times10^6$ M^{-1}, $1.01(\pm0.18)\times10^5 M^{-1}$and $1.11(\pm0.25)\times10^6$ M^{-1} corresponding to the complexes 1-4 respectively.

Table 3: Binding constant and number of binding sites for the interactions of Ni (II) thiocarboxamide complexes **1-4** with BSA.

System	K (M^{-1})	n
BSA+ complex 1	$5.12(\pm0.20)\times10^4$	1.09((±0.08)
BSA+ complex 2	$4.13(\pm0.35)\times10^4$	1.03(±0.05)
BSA+ complex 3	$1.82(\pm0.17)\times10^3$	0.88(±0.12)
BSA+ complex 4	$2.93(\pm0.06)\times10^5$	1.19(±0.10)

Binding analysis

When small molecules bind independently to a set of equivalent sites on a macromolecule, the equilibrium between free and bound molecules is represented by the Scatchard equation(4)[46, 47]:

$$\log[F_O\text{-}F/F] = \log K + n \log[Q] \quad (4)$$

Where, K and n are the binding constant and the number of binding sites, respectively. The plot of Log $[F_O\text{-}F/F]$ versus log [Q] can be used to determine the values of both K as well as n and such values calculated for complexes 1-4 shown in Fig.8 are listed in Table 3. From the values of n, it is clearly showed that there is only one independent class of binding sites for the complexes on BSA and also direct relation between the binding constant and number of binding sites. The fluorescence spectral result clearly shows that complex 4 having higher binding constant value when compared to other complexes.

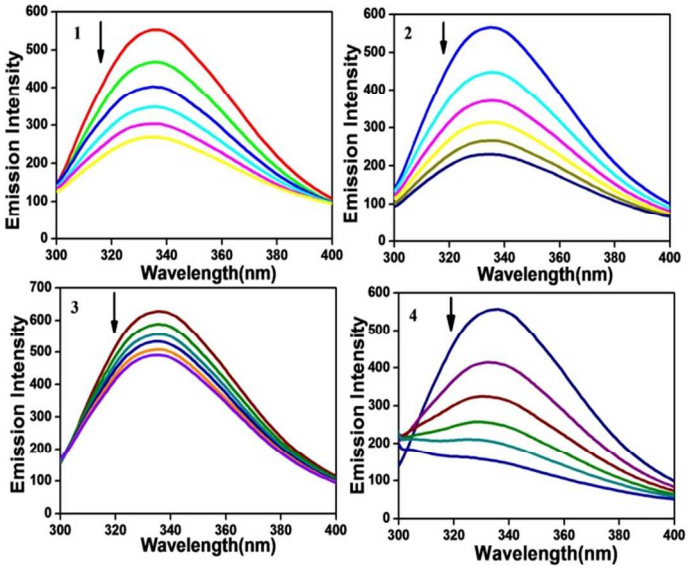

Fig: 7 The emission spectra of BSA at various concentration of complexes 1-4 [BSA]=1 μM and [complexes]=0-50 μM.

From K_{sv} values, the complex 4 exhibited stronger protein-binding ability with enhanced hydrophobicity. The complex 1 and 2 possess methyl substituent and complex 3 having trimethyl substituent will hindered the protein binding interactions and hence lower binding constant value. The larger value of K_{bin} and K_q indicates a strong interaction between the BSA and complexes. The calculated value of n is around 1 for all the complexes indicating the existence of just a single binding site in BSA for all the complexes. The result of binding constant value indicates that the complexes bind to BSA in the order of complexes **4>1>2>3.** Among the four nickel(II) thiocarboxamide complexes, the complex **4** has stronger interaction with BSA than the other nickel(II) thiocarboxamide complexes.

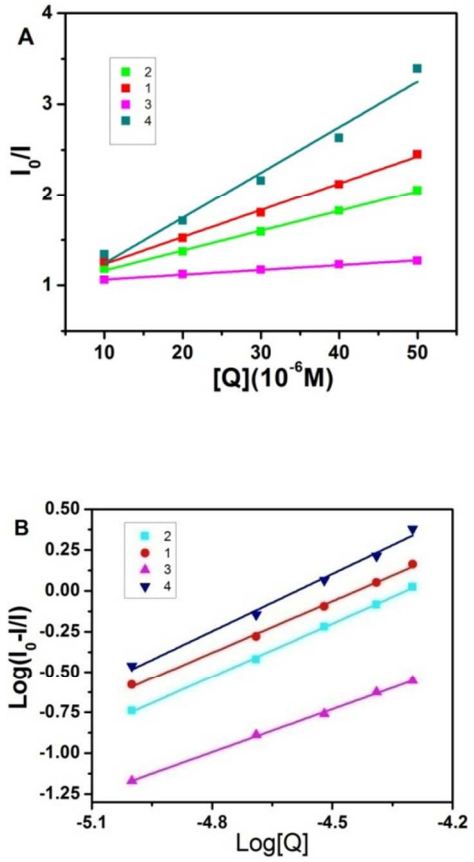

Fig: 8 The Stern-Volmer plots (A) and Scatchard plots (B) of the Luminescence titration of complexes **1-4** with BSA.

UV-visible absorption studies

UV-visible absorption measurement is the simple method is applicable to explore the structure changes and know the complex formation in the donor-acceptor systems. Quenching can occur by different mechanisms which are usually classified as static quenching and dynamic quenching. Static quenching refers to flurophore-quencher complex formation in the ground state while dynamic quenching refers to a process in which the flurophore and the quencher come into contact during transient existence of the excited state and the absorption spectra of the fluorescent substance is not changed. The UV absorption spectrum of pure BSA and BSA-complex (1-4) are shown in Fig.9. It is clearly shows that, the absorption band of BSA appeared at 280 nm has been increased after the addition of complexes. This illustrates that the interaction between BSA and complexes is a static one and it was involved in the formation of the ground state complex of the type BSA-complex. But, dynamic quenching affects only the excited state while it has no function on the absorption spectrum. Therefore, the mechanism is only static quenching was observed in the nickel(II) thiocarboxamide complexes. A similar type of static interaction between proteins with complexes has been previously reported.[48]

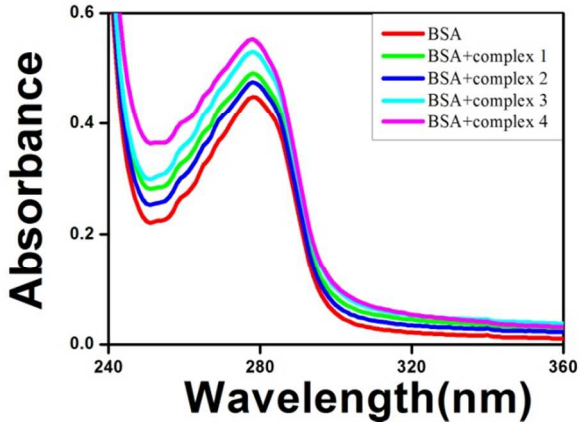

Fig: 9 The absorption spectra of BSA (1×10^{-5} M) in the presence of complexes **1-4** (5μM).

Characteristics of synchronous fluorescence spectra

To explore the structural changes of BSA upon the addition of nickel(II) thiocarboxamide complexes. After having obtained binding constant and number of binding sites with BSA, it is very important to know conformational changes of protein molecular environment. Thus we measured synchronous florescence spectra of BSA before and after the addition of nickel(II) thiocarboxamide complexes to get useful information on the micro environment, particularly in the vicinity of the flurophore functional groups.[49] It is well known fact that the fluorescence of protein is normally due to the presence of tyrosine, tryptophan and phenylalanine residues and hence spectroscopic methods are usually applied to investigate the conformational changes of serum protein. Among them tryptophan is the most dominant flurophore, located at the substrate binding sites. Most of the drugs bind to the protein in the active binding sites. Hence, synchronous method is usually applied to study the conformational changes in the active binding sites on the protein that is around the tyrosine and tryptophan region.

According to Miller[50], the difference between the excitation and emission wavelength indicates the type of chromophores. If the Δλ is small 15 nm the synchronous fluorescence spectra of BSA is characteristics of tyrosine residue whereas is used, the obtained synchronous spectrum indicated the spectral property of tyrosine larger Δλ value of 60 nm is characteristics of tryptophan residue[51]. The maximum emission wavelength of tryptophan and tyrosine residues in the protein molecule are related to the polarity of their surroundings, changes of the maximum emission wavelengths can reflect changes of protein conformation.

The synchronous fluorescence spectra of BSA upon the addition of nickel(II) thiocarboxamide complexes recorded with two different Δλ values i.e., Δλ=15 and 60 nm are shown in Fig 10 and 11. When Δλ=15 nm, it become clear that an increase in the concentration of the complexes added to BSA solution

increases the emission intensity. But in the case of Δλ=60 nm a significant decrease in the intensity of the synchronous spectral band was observed which indicates that the complexes affected the tryptophan residues. Though all the complexes affected both the microenvironments i.e.,tyrosine and tryptophan residues, the effect was more towards tryptophan than tyrosine residues. The interaction of the nickel(II) thiocarboxamide complexes with residues led to a decrease in the polarity of the fluorophore by an increasing the hydrophobicity around the same. Moreover, the strong interaction between the complexes with BSA demonstrates that these complexes can easily stored in protein and can be released in desired targets. The characretrics of the synchronous fluorescence measurements show the conformational changes occurred in BSA upon interaction with nickel(II) thiocarboxamide complexes.

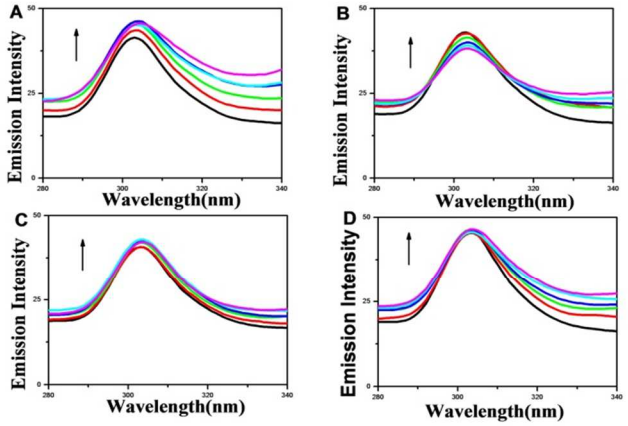

Fig:10 The Synchronous fluoresence spectra of BSA(1μM) as a function of concentrationof complex**1**(A), **2**(B), **3**(C),and **4**(D)(0-50μM) with a wave length difference of Δλ=15 nm.

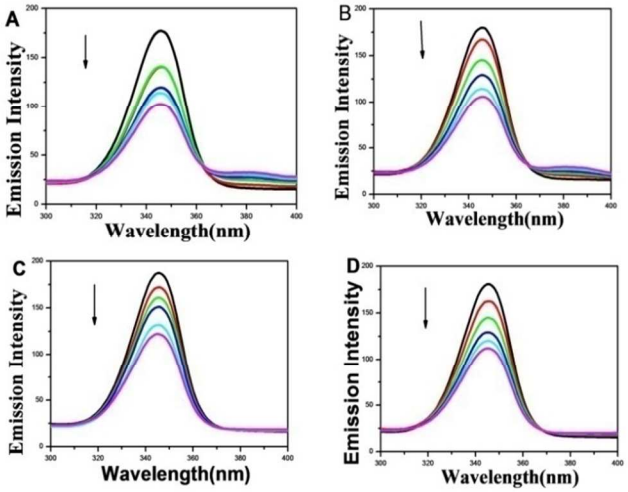

Fig: 11 The Synchronous fluoresence spectra of BSA(1μM) as a function of concentration of complexs 1(A), 2(B), 3(C),and 4(D)(0-50μM) with a wave length difference of Δλ=60 nm.

Antioxidant activity

Since the nickel(II) thiocarboxamide complexes exhibit good DNA and protein binding ability, it was further considered to study their ability to quench the free radical and antioxidant properties of the complexes. Hence we carried out experiments to investigate the free radical scavenging ability of the ligands, metallic precursors and nickel(II) thiocarboxamide complexes 1-4 against standard antioxidant BHT with DPPH, OH and NO radicals (Fig.12). It is to be noted that no significant radical scavenging activities were observed for ligands and the metallic precursors under the same experimental conditions. From the experimental results the IC_{50}value of the complexes with respect to DPPH, OH and NO radicals assays were found to be 25, 27.5, 30, 33μM , 27.5, 31.4, 34.2, 37 μM, 29.2, 31.5, 36.2 and 38μM respectively. The IC_{50} values show that the complexes exhibit antioxidant activity in the order of **1**> **2** > **3** > **4** > ligand> precursors in all of the experiments. The complexes 1-4 displayed almost comparable free radical scavenging activity with respect to the standard antioxidant (BHT). The results obtained against different radicals prove that the complexes are more effective to arrest the formation of the DPPH, OH radicals than that of NO radicals studied. The nickel complexes having higher antioxidant activity when compared to free ligand and metallic precursors, which shows that, the nickel(II) chelation plays an important role in determining the antioxidant properties. Among the complexes, complex 1 shows excellent radical scavenging activity and this might be due to the more electron donating nature and the planarity of the phenyl group. The lowest activity was observed for complex 3 due to the steric nature of trimethyl groups. So, the various antioxidant assay results clearly indicate that all the complexes are responsible for the scavenging activity. The lower IC_{50} values observed in antioxidant assays did explain these complexes have a strong potential to be used as scavengers to eliminate free radicals.

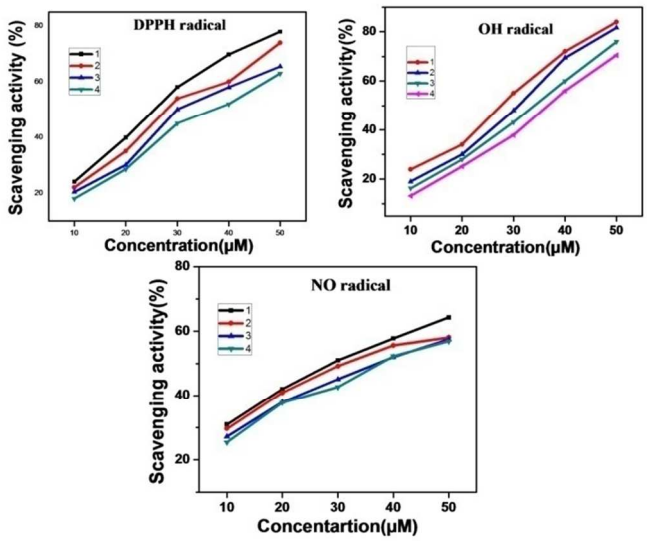

Fig:12 Trends in the inhibition of radicals by complexes.

In vitro cytotoxicity

In recent years considerable effort has been taken to develop of nickel(II) complexes as potential anticancer agents.[52] The metallic precursors, ligand and nickel(II) thiocarboxamide complexes(1-4) were evaluated for their cytotoxic activity against HeLa, MG63 and NIH-3T3 cell lines by using calorimetric assay (MTT assay) that measures mitochondrial dehydrogenase activity as an indication of cell viability. Complexes 1-4 were dissolved in DMSO and blank samples containing the same amount of DMSO are taken as controls. The cells were treated with various concentrations of the test compound. The effects of the nickel(II) complexes to arrest the proliferation of cancer cells were evaluated after an exposure of 48 h. For comparison, the cytotoxicity of the well known anti-cancer drug cisplatin against all the above cell lines.

The results were studied by means of cell viability curves and expressed with values in the studied concentration range from 0.1-100 μM. The activity corresponding to inhibition of cancer cell growth at maximum level as expressed as IC_{50} values were related to inhibition of cancer cell growth at the 50% level, are noted.

It is to be noted that the precursor and the ligand did not show any inhibition of the cell growth even up to100 μM and clearly indicates chelation of the ligand with metal ion is responsible for the observed cytotoxicity properties of the complexes. The results of MTT assays revealed that complexes showed notable activity against both the cell lines HeLa and MG63 with respect to IC_{50} values is represented in Table.4. The cytotoxic activity of the complex 3 is found to be very superior when compared to other complexes. The observed higher efficiency of the complex 3 is correlated to the nature of the substitution of the thiocarboxamide ligand coordinated to the nickel ion in it. The higher cytotoxicity is observed for complex 3 which containing three methyl groups causes the electron delocalization on the aromatic ring system and subsequently increases the lipophilic character of the metal complex which favours its permeation through the lipid layer of the cell membrane. Among the two different cell lines used in that is study, the proliferation of HeLa cell lines was arrested to a greater extent than MG63 cells by the complexes. Though the above mentioned complexes are active against the cell lines under in vitro cytotoxicity experiments, none of the complexes could reach the effectiveness shown by the standard drug cisplatin (IC_{50} value 35.20 and 32.16μM, respectively). The in vitro cytotoxic activity have also shows that the IC_{50} value of complex against NIH-3T3 (non-cancerous cells) is found to be above 200 μM did not show any damage to normal cells. The results of the cell viability tests imply that the complexes 1-4 have the ability to arrest the proliferation of cancer cells without causing any damage to the normal cells. The IC_{50} values of the present complexes are much better than those previously reported nickel complexes.[53]

Table 4: The cytotoxic activity of the complexes.[a]IC_{50} values (μM)

Complex	HeLa	MG63	NIH-3T3
1	>100	>100	231.78±2.40
2	78.81±0.50	109.4±0.20	234.26±1.78
3	41.97±0.48	53.19±0.29	255.91±1.18
4	62.74±0.26	>100	247.22±2.98
Cisplatin	35.20±0.50	32.16±0.58	240.15±0.98

[a]IC_{50}= Concentration of the drug required to inhibit growth of 50% of the cancer cells (μM).

Conclusion

An easy route to synthesis nickel(II) complexes bearing thiocarboxamide ligands has been described. The DNA binding properties of nickel(II) thiocarboxamide complexes were examined by the absorption and emission spectra, which suggest their involvement in intercalative DNA interaction with different binding affinities. The binding constants showed that the DNA binding ability increased in the order of **1>2>3>4**. All complexes cleave DNA with supercoiled form into nicked circular form. The circular dichronic spectral result confirms intercalative mode of binding between the CT-DNA with complexes and the DNA conformational changes was not observed. The protein binding of the complexes was studied by the fluorescence spectral methods indicate the binding affinity increases based on the substitution in the phenyl ring at the terminal nitrogen. Further, the protein biding results reveal that nickel complexes show high binding affinity with the serum albumins and quench the fluorescence of serum albumins through a static quenching mechanism. All the complexes exhibit excellent radical scavenging abilities and showed greater IC_{50} values. The cytotoxic study reveals that all the complexes show better cytotoxicity against HeLa and MG 63 cell lines and complex 3 shows the highest anti cancer activity among them. The present work describes the significant role of nickel(II) complexes in the studies of DNA/ protein binding, antioxidant and cytotoxicity activities.

Experimental

Materials and Instrumentation

Nickel(II) acetate tetrahydrate, 2-methyl pyridine, sulfur, aniline derivatives were purchased from Merck and Aldrich chemicals and used as received. Solvents were dried and freshly distilled prior to use. Calf-thymus DNA (CT-DNA) and ethidium bromide (EtBr) purchased from Sigma-Aldrich chemie were uses as received. Bovine serum albumin (BSA) was purchased from Himedia Company. 3-(4, 5-Dimethylthiazol-2-yl)-2, 5-diphenyltetrazolium bromide (MTT) were purchased from Sigma-Aldrich and used as received. Human cervical cancer cells were obtained from National

centre for cell Science (NCCS), Pune, India. All other chemicals and reagents used for the biological studies were of high quality in biological grade. Elemental analyses were performed on a vario EL III CHNS elemental analyser. Melting points were performed with an electrical instrument and are uncorrected. Infrared spectra were recorded in KBr pellets with a JASCO 200 plus spectrometer. The ^{1}H-NMR and ^{13}C-NMR were recorded on a high resolution Bruker 400 MHz instrument and the chemical shifts given in ppm are referenced to the deuterated solvents. Electronic spectroscopy was recorded with a Cary 300 Bio Varian spectrophotometer using cuvettes of 1 cm path length. Emission intensity measurements were carried out using a Jasco FP-6500 spectrofluorimeter. The circular dichromism spectra were recorded using a JASCO J-810 spectropolarimeter equipped with a peltier Temperature control device at room temperature with a quartz cell of 1cm path length. Each sample solution was the average of 3 accumulations using a scan speed of 500 nm/ min at 1s response time. The viscosity measurements were carried out on a Schott Gerate AVS 310 viscometer at 30.0±0.1 °C in a thermostatic waterbath.

Preparation of thiocarboxamide ligands

The bidentate thiocarboxamides ligands (L1-L4) were prepared by reported procedure.[54] A mixture of substituted aniline (0.10 mol), sulfur (0.30 mol) and sodium sulfide nonahydrate (2 mol %) in 2-methylpyridine (60 mL) was refluxed for 48 h. After cooling and removal of all volatiles in vacuum, the dark solid residue was taken up in dichloromethane (200 mL), and the mixture was filtered through a column of silica gel. The filtrate was evaporated under reduced pressure, and the resulting solid was dried in vacuum. Recrystallisation from ethanol gave yield (74-79%) of analytically pure thiocarboxamide ligands as a yellow to orange crystalline solid.

N-(2-Methylphenyl)pyridine-2-thiocarboxamide(L1):
Yellow; Yield: 75%; M.p. 99-101°C. $C_{13}H_{12}N_2S$ (228.31): calcd. C 68.39, H 5.30, N 12.27, S 14.04; found C 68.10, H 5.58, N 12.40, S 13.01. ^{1}H NMR (400 MHz, $CDCl_3$): δ = 2.1 (s, 3 H, $PhCH_3$), 7.26 (d, ^{3}J=8.4 Hz, 2 H, 3- and 5-PhH), 7.46 (ddd, $^{3}J_{4,5}$ = 7.7, $^{3}J_{5,6}$ = 4.8, $^{4}J_{3,5}$ = 1.2 Hz, 1 H, 5-PyH), 7.87 (dt, $^{3}J_{3,4}$ =$^{3}J_{4,5}$ =7.7, $^{4}J_{4,6}$ = 1.8 Hz, 1 H, 4-PyH), 7.93 (d, ^{3}J =8.4 Hz, 2 H, 2- and 6-PhH), 8.54 (ddd, $^{3}J_{5,6}$ = 4.8, $^{4}J_{4,6}$ =1.8, $^{5}J_{3,6}$ = 0.9 Hz, 1 H, 6-PyH), 8.80 (ddd, $^{3}J_{3,4}$=7.7, $^{4}J_{3,5}$ = 1.2, $^{5}J_{3,6}$=0.9 Hz, 1 H, 3-PyH), 11.99 (br. s, 1 H, CSNH) ppm. IR (KBr): ν = 3310, 898 cm^{-1}.

N-(4-Methylphenyl)pyridine-2-thiocarboxamide(L2):
Yellow; Yield: 79%; M.p. 110-112°C. $C_{13}H_{12}N_2S$ (228.31): calcd. C 68.39, H 5.30, N 12.27, S 14.04; found C 68.10, H 5.57, N 12.36, S 13. ^{1}H NMR (400 MHz, $CDCl_3$): δ = 2.38 (s, 3 H, $PhCH_3$), 7.26 (d, ^{3}J = 8.4 Hz, 2 H, 3- and 5-PhH), 7.46 (ddd, $^{3}J_{4,5}$ =7.7, $^{3}J_{5,6}$ = 4.8, $^{4}J_{3,5}$ = 1.2 Hz, 1 H, 5-PyH), 7.87 (dt, $^{3}J_{3,4}$ = $^{3}J_{4,5}$=7.7, $^{4}J_{4,6}$ =1.8 Hz, 1 H, 4-PyH), 7.93 (d, ^{3}J =8.4 Hz, 2 H, 2- and 6-PhH), 8.54 (ddd, $^{3}J_{5,6}$ = 4.8, $^{4}J_{4,6}$ = 1.8, $^{5}J_{3,6}$ = 0.9 Hz, 1 H, 6-PyH), 8.80 (ddd, $^{3}J_{3,4}$=7.7, $^{4}J_{3,5}$ = 1.2, $^{5}J_{3,6}$ =0.9 Hz, 1 H, 3-PyH), 11.99 (br. s, 1 H, CSNH) ppm. IR (KBr): ν = 3240, 820 cm-1.

N-(2,4,6-Trimethylphenyl)pyridine-2-thiocarboxamide(L3):
Yellow-brown; Yield:74%; M.p.117-119°C. $C_{15}H_{16}N_2S$ (256.37): calcd. C 70.28, H 6.29, N 10.93, S 12.51; found C 70.21, H 6.41, N 10.72, S 12.48. ^{1}H NMR (400 MHz, $CDCl_3$): δ = 2.22 (s, 6 H, 2- and 6-$PhCH_3$), 2.33 (s, 3H, 4-$PhCH_3$), 6.99 (s, 2 H, 3- and 5-PhH), 7.50 (ddd, $^{3}J_{4,5}$ = 7.7, $^{3}J_{5,6}$ =4.8, $^{4}J_{3,5}$ = 1.2 Hz, 1 H, 5-PyH), 7.89 (dt, $^{3}J_{3,4}$ = $^{3}J_{4,5}$ =7.7, $^{4}J_{4,6}$ = 1.8 Hz, 1 H, 4-PyH), 8.58 (ddd, $^{3}J_{5,6}$ = 4.8, $^{4}J_{4,6}$ = 1.8, $^{5}J_{3,6}$ = 0.9 Hz, 1 H, 6-PyH), 8.80 (ddd, $^{3}J_{3,4}$ = 7.7, $^{4}J_{3,5}$ = 1.2, $^{5}J_{3,6}$ = 0.9 Hz, 1 H, 3-PyH), 11.29 (br. s, 1 H, CSNH) ppm.IR (KBr): ν = 3274, 855 cm-1.

N-(2-Chlorophenyl)pyridine-2-thiocarboxamide(L4):
Orange; Yield: 74%; M.p. 93-95°C. $C_{12}H_9ClN_2S$ (248.75): calcd. C 57.94, H 3.64, N 11.26, S 12.86; found C 57.87, H 3.59, N 11.22, S 12.77. ^{1}H NMR (400 MHz, $CDCl_3$): δ = 7.26 (d, ^{3}J=8.4 Hz, 2 H, 3- and 5-PhH), 7.46 (ddd, $^{3}J_{4,5}$ = 7.7, $^{3}J_{5,6}$ = 4.8, $^{4}J_{3,5}$ = 1.2 Hz, 1 H, 5-PyH), 7.84 (dt, $^{3}J_{3,4}$ =$^{3}J_{4,5}$=7.7, $^{4}J_{4,6}$ = 1.8 Hz, 1 H, 4-PyH), 7.93 (d, ^{3}J =8.4 Hz, 2 H, 2- and 6-PhH), 8.45 (ddd, $^{3}J_{5,6}$ =4.8, $^{4}J_{4,6}$ = 1.8, $^{5}J_{3,6}$=0.9 Hz, 1 H, 6-PyH), 8.73 (ddd, $^{3}J_{3,4}$ =7.7, $^{4}J_{3,5}$ = 1.2, $^{5}J_{3,6}$ = 0.9 Hz, 1 H, 3-PyH), 10.38 (br. s, 1 H, CSNH) ppm.IR (KBr): ν = 3214, 840 cm^{-1}.

Synthesis of new square plannar nickel(II) thiocarboxamide complexes

All the reactions were carried out under unhydrous conditions and the new nickel(II) complexes were prepared by the following procedure[55]: To a solution of thiocarboxamide ligands (2mmol) (L1-L4) was added in ethanol under constant stirring. Solid $Ni(CH_3COO)_2{\cdot}4H_2O$ (1 mmol) was added and the solution was heated to refluxed for 5h. A yellow colored mononuclear nickel complex $[Ni(L)_2]$ precipitated. The solid was separated by the filtration and washed with ethanol and dried under vacuum. (Scheme: 1)

[Ni $(L1)_2$] (1)

Yield: 79.5%. M.P. 246°C Color: Yellow. Anal. Calc. for $C_{26}H_{22}N_4S_2Ni$: C; 60.84, H; 4.32, N; 10.91, S; 12.46. Found: C; 60.70, H; 4.39, N; 10.80, S; 12.31. IR (KBr, cm^{-1}) γ= 1620, 1202. UV-Vis in $CHCl_3$: $\boldsymbol{\lambda}_{max}$/nm ($\varepsilon_{max}$/dm^{3}mol^{-1}cm^{-1}) 241(70,280), 270(72,730), 344(5279), 466(1393). ^{1}H NMR (400 MHz, $CDCl_3$): 2.2 (s, CH_3, 6H), 7.01-7.14 (m, 8 H, Ar-H),7.76(d, 2H, 8.4 Hz), 7.73 (d, ^{3}J=8.4 Hz, 2H, PyH), 8.08 (d, ^{3}J =8.4 Hz, 2H, PyH), 8.10 (ddd, $^{3}J_{4,5}$ = 6.4, $^{3}J_{5,6}$ = 1.2, $^{4}J_{3,5}$ = 0.8 Hz, 2H, PyH), 8.28 (dt, $^{3}J_{3,4}$ =$^{3}J_{4,5}$ =4, $^{4}J_{4,6}$ = 0.8 Hz, 2H, PyH) ppm.δ_c(100MHz) 167.68, 162.92, 152.76, 149.81, 138.50, 130.43, 128.59, 126.22, 125.81, 124.10, 122.81, 118.99,17.92 ppm.

[Ni $(L2)_2$] (2)

Yield: 91.7%. M.P.250°C Color: Yellow. Anal. Calc. for $C_{26}H_{22}N_4S_2Ni$: C; 60.84, H; 4.32, N; 10.91, S; 12.46. Found: C; 60.72, H; 4.29, N; 10.81, S; 12.52. IR (KBr, cm^{-1}) γ= 1634, 1218. UV-Vis in $CHCl_3$: $\boldsymbol{\lambda}_{max}$/nm ($\varepsilon_{max}$/dm^{3}mol^{-1}cm^{-1}) 242(59,080), 267(60,140), 350(4613), 472(1296). ^{1}H NMR

(400 MHz, $CDCl_3$): 2.3 (s, CH_3, 6H), 7.10-7.14 (m, 8 H, Ar-H),7.26(d, 2H, 8.4 Hz, PyH), 7.73 (d, ^3J=7.2 Hz, 2H, PyH), 8.08 (d, ^3J =8.4 Hz, 2H, PyH), 8.10 (ddd, $^3J_{4,5}$ = 6.4, $^3J_{5,6}$ = 1.2, $^4J_{3,5}$ = 0.8 Hz, 2H, PyH) 8.07 (dt, $^3J_{3,4}$ =$^3J_{4,5}$ =6.8, $^4J_{4,6}$ = 1.2 Hz, 2H, PyH), 8.30 (dt, $^3J_{3,4}$ =$^3J_{4,5}$ =5.2, $^4J_{4,6}$ = 0.8 Hz, 2H, PyH) ppm. δ_c(100MHz) 167.67, 163.45, 152.63, 148.24, 138.39, 133.90, 129.49, 125.66, 122.77, 120.97, 21.16 ppm.

[Ni $(L3)_2$] (3)

Yield: 92.73%. M.P.280°C Color: Yellow. Anal. Calc. for $C_{30}H_{30}N_4S_2Ni$: C; 63.29, H; 5.31, N; 9.83, S; 11.24. Found: C; 63.19, H; 5.29, N; 9.82, S; 11.28. IR (KBr, cm^{-1}) γ= 1620, 1259. UV-Vis in $CHCl_3$: $\boldsymbol{\lambda}_{max}$/nm ($\varepsilon_{max}$/$dm^3mol^{-1}cm^{-1}$) 237(78,330), 266(80,440), 340(5490), 467(1204). ^{1}H NMR (400 MHz, $CDCl_3$): 2.3 (s, CH_3, 6H),2.1(s, CH_3, 3H), 6.92-7.12 (m, 4H, Ar-H),7.26(d, 2H, 8.4 Hz, PyH), 7.77 (dt, $^3J_{3,4}$ =$^3J_{4,5}$ =6.0, $^4J_{4,6}$ = 1.6 Hz, 2H, PyH), 7.77 (d, ^3J=8.4 Hz, 2H, PyH), 8.12 (dt, $^3J_{3,4}$ =$^3J_{4,5}$ =6.8, $^4J_{4,6}$ = 1.2 Hz, 2H, PyH) 8.28 (ddd, $^3J_{4,5}$ = 5.2, $^3J_{5,6}$ = 0.8, $^4J_{3,5}$ = 0.4 Hz, 2H, PyH), ppm. δ_c(100MHz) 167.83, 162.40, 152.96, 146.18, 138.49, 132.57, 128.55,126.17, 125.76, 122.77, 20.95, 17.95 ppm.

[Ni $(L4)_2$] (4)

Yield: 75.33%. M.P. 258°C Color: Yellow. Anal. Calc. for $C_{24}H_{16}N_4S_2Cl_2Ni$: C; 52.02, H; 2.91, N; 10.11, S; 11.57. Found: C; 51.98, H; 2.89, N; 10.04, S; 11.48. IR (KBr,cm^{-1}) γ= 1612, 1210. UV-Vis in $CHCl_3$: $\boldsymbol{\lambda}_{max}$/nm ($\varepsilon_{max}$/$dm^3mol^{-1}cm^{-1}$) 241(70,630), 269(75,880), 348(5454), 470(1324). ^{1}H NMR (400 MHz, $CDCl_3$): 7.07-7.18 (m, 8H, Ar-H),7.31(d, 2H, 8.0 Hz, PyH), 7.48(d, 2H, 7.2 Hz, PyH), 8.13 (dt, $^3J_{3,4}$ =$^3J_{4,5}$ =6.8, $^4J_{4,6}$ = 0.8 Hz, 2H, PyH), 7.31(d, 2H, 8.0 Hz, PyH), 8.27 (d, ^3J=4 Hz, 2H, PyH), ppm. δ_c(100MHz) 170.40, 162.57, 152.74, 148.15, 138.79, 129.89, 127.18, 126.15, 125.33, 124.95, 123.18, 121.22 ppm.

X-ray crystallography

Single crystals of complex 1 suitable for X–ray diffraction analysis were obtained by slow evaporation of dimethyl formamide solution of the complex at room temperature. The data collection was carried out using Bruker SMART APEX II single crystal X–ray diffractometer using monochromated Mo K_α radiation (kI = 0.71073 Å). The absorption corrections were performed by multi-scan method using SADABS software.[56] Corrections were made for Lorentz and polarization effects. The structures were solved by SIR92[57] and refined by full–matrix least squares on F^2 using SHELXL 97.[58] All non–hydrogen atoms were refined anisotropic ally and the hydrogen atoms in these structures were located from the difference Fourier map and constrained to the ideal positions in the refinement procedure. The unit cell parameters were determined by the method of difference vectors using reflections scanned from three different zones of the reciprocal lattice. The intensity data were measured using ω and φ scan with a frame width of 0.5°. Frame integration and data reduction were performed using the Bruker SAINT–Plus (Version 7.06a) software.[59] The crystal structure and structure refinement parameters for the structure is given in the Table 1.

DNA binding studies

UV-visible titration method was performed to study the binding interaction of complexes with CT-DNA. All experiments involving calf-thymus DNA (CT-DNA) were performed with a Tris-HCl buffer solution (p^H=7.2).The concentration of CT-DNA was measured by UV absorbance at 260 nm. A stock solution of CT-DNA was stored at 277 K and used after no more than 4 days. In electronic absorption titration experiments were performed by keeping the concentration of metal complex as constant and varying the nucleotide concentration. While doing the absorption spectra, equal amounts of DNA were added to both complexes and reference solutions to eliminate the absorbance of DNA itself. The data were applied into the following equation and the intrinsic binding constant K_b was calculated using the following equation,

$$[DNA] / [\varepsilon_a-\varepsilon_f] = [DNA] / [\varepsilon_b-\varepsilon_f] + 1/K_b [\varepsilon_b-\varepsilon_f]$$

Where, [DNA] is the concentration of DNA in base pairs, ε_a is the extinction coefficient of the complex at a given DNA concentration, ε_f is the extinction coefficient of the complex in free solution and ε_b is the extinction coefficient of the complex when fully bound to DNA. A plot of [DNA]/ $[\varepsilon_b-\varepsilon_f]$ versus [DNA] gave a slope and intercept equal to 1/ $[\varepsilon_b-\varepsilon_f]$ and $(1/K_b)$ $[\varepsilon_b-\varepsilon_f]$, respectively. The intrinsic binding constant K_b is the ratio of the slope to the intercept.

Luminescence titration in the presence of Ethidium bromide

The competitive interaction of all the complexes was studied by fluorescence spectral technique in order to find out whether the compound can displace EB from its DNA-EB complex. Ethidium bromide displacement experiments were done by adding the solution of the complexes to the Tris-HCl buffer solution (p^H, 7.2) of DNA/EB mixture. Before starting measurements, the mixture was shaken up and recorded. The changes in fluorescence intensities of EB bound to DNA were measured with respect to different concentration of the complex. EB was non-emissive in Tris-HCl buffer solution (p^H, 7.2) due to florescence quenching of free EB by the solvent molecules. In the presence of DNA, EB showed enhanced intensity due to its intercalative binding to DNA. A competitive interaction of the metal complexes to CT DNA resulted in the displacement of the bound EB thereby decreasing its emission intensity. The quenching constant (K_q) was calculated using the classical Stern-Volmer equation:

$$I_0/I = K_q [Q] + 1$$

Where $I_0$is the emission intensity of the absence of quencher, I is the emission intensity of the presence of quencher, K_q is the quenching constant, [Q] is the quencher concentration. K_q is the slope obtained from the plot of I_0/I versus [Q].Further the apparent binding constant (K_{app}) was calculated from the following equation:

$$K_{EtBr} [EtBr] = K_{app} [complex]$$

(Where the complex concentration was obtained from the value at a 50% reduction of the fluorescence intensity of EtBr, K_{EtBr}= 1.0×10^7 M^{-1} and [EtBr] =10μM.

DNA cleavage experiments

The DNA cleavage ability of the complexes was monitored by using gel electrophoresis techniques. A solution containing 25μL of pUC19 DNA (1μg), Tris-HCl (50 μM, p^H, 7.5), NaCl (50 mM), the metal complexes (35μM) and H_2O_2(60μM) was incubated at 37°C for 1h. Subsequently , 4μL of 6X DNA loading buffer containing 0.25% bromophenol blue, 0.25% xylene cyanol and 60% glycerol was added to the test solution and then mixed with 1% agarose containing the 1.0 μg mL^{-1} of ethidium bromide. Electrophoresis was done at 5 Vcm^{-1} for 2h in a Tris-Acetate-EDTA(TAE) buffer and the bands were visualized in a Gel doc system and photographing the fluorescence of intercalated ethidiumbromide under a UV illuminator.The intensity of each band relative to that of the plasmid supercoiled form was multiplied by 1.43 to take account of the reduced affinity for ethidium bromide.[60] The cleavage ability was determined based on the ability of the complex to convert the supercoiled form (Form-I) in to nicked circular form (Form-II).

Circular dichroism spectral study

CD spectroscopic technique is very helpful to ascertain the conformational changes induced by the interaction of drugs as well as destablisation of the DNA helix. The B-form conformation of DNA showed two consecutive CD bands in the UV region, a positive band at 275 nm due to base stacking and a negative band at 246 nm due to polynucleotide helicity. The conformational changes are tested by upon the addition of complexes (20μM) with DNA concentration at 60 μM in Tris-HCl buffer medium. The spectrum of control DNA and the complexes was monitored from 220 to 320 nm. It is known that changes in ellipticity are directly related to the conformational changes observed in circular dichroism. The changes in CD signals of DNA observed on interaction with drugs may often be assigned to the corresponding changes in the DNA structure.[61] Thus, simple groove binding and electrostatic interaction of small molecules show less or no perturbation on the base-stacking and helicity bands, while intercalation enhances the intensities of both the bands stabilizing the right-handed B conformation of DNA as observed for the classical methylene blue.[62]

Viscosity experiments

The viscosity measurements were carried out on a Schott Gerate AVS 310 viscometer at 30.0±0.1 °C in a thermostatic waterbath. Calf thymus DNA sample solutions were prepared by sonication inorder to mimimize complexities arising from DNA flexibility.[63] The CT-DNA solution (5 μM) was titrated with nickel(II) complexes (0.5-5 μM), following the change of the viscosity in each case. Flow time was measured with a digital stopwatch and each sample was measured at least for three times, and an average flow time was calculated. Data are presented as $(\eta-\eta_o)^{1/3}$ versus binding ratio, where η is the viscosity of DNA in the presence of the complex, and η_o is the viscosity of DNA alone. The relative viscosity values was calculated according to the relation $\eta = (t - t_o)/t_o$, where t_o is the total flow time for the buffer and t is the observed flow time for DNA in the presence and absence of the complex.[64]

Protein binding studies

Protein binding study of nickel(II) thiocarboxamide complexes with bovine serum albumin (BSA) was studied using fluorescence spectra were recorded with an excitation at 280 nm and the emission wavelength at 345 nm corresponding to that of free bovine serum albumin (BSA). The excitation and emission slid widths and scan rates were constantly maintained for all the experiments. Samples were carefully degassed using pure nitrogen gas for 15 minutes by using quartz cells (4×1×1cm) with high vacuum Teflon stopcocks. Stock solutions of BSA was prepared in 50mM phosphate buffer (p^H, 7.2) and stored in dark at 4°C for further use. Concentrated stock solutions of metal complexes were prepared by dissolving them in DMSO: phosphate buffer (5:95) and diluted suitably with phosphate buffer to get required concentrations. A 2.5 mL solution of BSA (1 μM) was titrated by successive additions of a 25μL stock solution of complexes (10^{-3}M) using a micropipette. Synchronous florescence spectra was also recorded using the same concentration of BSA and complexes as mentioned above with two different Δλ (difference between the excitation and emission wavelengths of BSA) values such as 15 and 60 nm.

Antioxidant activity

The DPPH, OH and NO radical scavenging activities of the metal complexes were determined by the methods described by Blois, Nash and Green et al., respectively.[65, 66, 67]for each of the above assay, tests were done in triplicate by varying the concentration of the complexes ranging from 10-50μM. The percentage activity was calculated by using the formula, % activity = $[(A_o-A_c/A_o)\times100$, where A_o and A_c represent the absorbance in the absence and presence of the test compounds respectively. The 50% activities (IC_{50}) were calculated from the results of percentage activity.

In vitro anticancer activity: Maintenance of cell lines

The tests were done in monolayer cells were detached with trypsin-ethylenediaminetetraacetic acid (EDTA) to make single cell suspensions and viable cells were counted using a hemocytometer and diluted with medium containing 5% FBS to give final density of 1×10^5 cells/ml. One hundred microlitres per well of cell suspension were seeded into 96-well plates at plating density of 10,000 cell/well and incubated to allow for cell attachment at 37°C, under conditions of 5% CO_2, 95% air and 100% relative humidity. After 24 h the cells were treated with serial concentration of the test samples. The compounds were initially dissolved in neat DMSO and an aliquot sample solution was diluted to twice the desired final maximum test concentration with serum free medium. Additional four serial

dilutions were made to provide a total of five sample concentrations. Aliquots of 100 µL of these different sample dilutions were added to the appropriate wells already containing 100µL of medium, resulting in the required final sample concentrations. Following sample addition, the plates were incubated for an additional 48 h at 37 °C 5% CO_2, 95% air and 100% relative humidity. The medium containing without samples were served as control and triplicate was maintained for all concentrations.

MTT assay

3-[4, 5-dimethylthiazol-2-yl] 2, 5-diphenyltetrazolium bromide (MTT) is a yellow water soluble tetrazolium salt. A mitochondrial enzyme in living cells, succinate dehydrogenase, cleaves the tetrazolium ring, converting the MTT to an insoluble purpule formazan.[68] Therefore, the amount of formazan produced is directly propotional to the number of viable cells. After 48 h incubation, 15 µL of MTT (5 mg mL^{-1}) in phosphate buffered saline (PBS) was added to each well and incubated at 37 °C for 4h. The medium with MTT was then flicked off and the formed formazan crystals were solubilized in 100 µL of DMSO and then measured the absorbance at 570 nm using micro plate reader. Non linear regression graph was plotted between % cell inhibition and Log concentration and IC_{50} value was determined using GraphPad prism software. The % cell inhibition was determined using the following formula, % cell inhibition=100-Abs (sample)/Abs (control) ×100 The IC_{50} values were determined from the graph plotted between % cell inhibition and concentration.

Acknowledgements

One of the authors (R.R.K) thank DST, India, for the award of DST-INSPIRE Fellowship. We thank UGC-SAP and DST-India (FIST programme) for the use of Bruker 400 MHz NMR and fluorescence spectral facilities at the School of chemistry, Bharathidasan University. We also thank Dr. S. Sanjib karmakar, Guwahati University, for collecting single crystal X-ray diffraction data.

References

1. Y.-J. Liu, N. Wang, W.-J. Mei, F. Chen, L.-X. He, L.-Q. Jian, R.-J. Wang and F.-H. Wu, *Transition Metal Chemistry*, 2007, **32**, 332-337.
2. G. Zuber, J. C. Quada and S. M. Hecht, *Journal of the American Chemical Society*, 1998, **120**, 9368-9369.
3. E. R. Jamieson and S. J. Lippard, *Chemical Reviews*, 1999, **99**, 2467-2498.
4. I. Meistermann, V. Moreno, M. J. Prieto, E. Moldrheim, E. Sletten, S. Khalid, P. M. Rodger, J. C. Peberdy, C. J. Isaac, A. Rodger and M. J. Hannon, *Proceedings of the National Academy of Sciences of the United States of America*, 2002, **99**, 5069-5074.
5. R. Trondl, P. Heffeter, C. R. Kowol, M. A. Jakupec, W. Berger and B. K. Keppler, *Chemical Science*, 2014, **5**, 2925-2932.
6. S. H. van Rijt and P. J. Sadler, *Drug Discovery Today*, 2009, **14**, 1089-1097.
7. H. Mansouri-Torshizi, M. Saeidifar, F. Khosravi, A. Divsalar, A. A. Saboury and F. Hassani, *Bioinorganic Chemistry and Applications*, 2011, **2011**, 394506.
8. D. Palanimuthu, S. V. Shinde, K. Somasundaram and A. G. Samuelson, *Journal of Medicinal Chemistry*, 2013, **56**, 722-734.
9. P. Sathyadevi, P. Krishnamoorthy, N. S. P. Bhuvanesh, P. Kalaiselvi, V. Vijaya Padma and N. Dharmaraj, *European Journal of Medicinal Chemistry*, 2012, **55**, 420-431.
10. H. Cheng, H. Liu, Y. Zhang and G. Zou, *Journal of Luminescence*, 2009, **129**, 1196-1203.
11. K. S. Ghosh, S. Sen, B. K. Sahoo and S. Dasgupta, *Biopolymers*, 2009, **91**, 737-744.
12. M. Ristow and K. Zarse, *Experimental Gerontology*, 2010, **45**, 410-418.
13. G. Bjelakovic, D. Nikolova, L. Gluud, R. G. Simonetti and C. Gluud, *Journal of American Medical Association*, 2007, **297**, 842-857.
14. J. K. Willcox, S. L. Ash and G. L. Catignani, *Critical Reviews in Food Science and Nutrition*, 2004, **44**, 275-295.
15. I. Björkhem, A. Henriksson-Freyschuss, O. Breuer, U. Diczfalusy, L. Berglund and P. Henriksson, *Arteriosclerosis, Thrombosis, and Vascular Biology*, 1991, **11**, 15-22.
16. U. Ermler, W. Grabarse, S. Shima, M. Goubeaud and R. K. Thauer, *Current Opinion in Structural Biology*, 1998, **8**, 749-758.
17. B. E. Barton and T. B. Rauchfuss, *Journal of the American Chemical Society*, 2010, **132**, 14877-14885.
18. Z. Lu, C. White, A. L. Rheingold and R. H. Crabtree, *Inorganic Chemistry*, 1993, **32**, 3991-3994.
19. i. J. R. L. E. R. Cammac, *The Bioinorganic Chemistry of Nickel*, VCH, New York, 1988.
20. H. G. W. S.W. Ragsdale, J.A. Morton, L. G. Ljungdhal, D. V. Dervartanian, in: J.R. Lanscater Jr.(Ed) *The Bioinorganic Chemistry of Nickel*, VCH, New York, 1988.
21. P. li, M. Niu, M. Hong, S. Cheng and J. Dou, *Journal of Inorganic Biochemistry*, 2014, **137**, 101-108.
22. N. Selvakumaran, N. S. P. Bhuvanesh, A. Endo and R. Karvembu, *Polyhedron*, 2014, **75**, 95-109.
23. P. Kalaivani, S. Saranya, P. Poornima, R. Prabhakaran, F. Dallemer, V. Vijaya Padma and K. Natarajan, *European Journal of Medicinal Chemistry*, 2014, **82**, 584-599.
24. T. Kanbara, K. Okada, T. Yamamoto, H. Ogawa and T. Inoue, *Journal of Organometallic Chemistry*, 2004, **689**, 1860-1864.
25. K. P. Deepa and K. K. Aravindakshan, *Synthesis and Reactivity in Inorganic and Metal-Organic Chemistry*, 2000, **30**, 1601-1616.
26. K. Nakamoto, *Infrared and Raman Spectra of Inorganic and Coordination compounds*, Wiley Interscience, New York, 1971.

27. O. Rotthaus, F. Thomas, O. Jarjayes, C. Philouze, E. Saint-Aman and J.-L. Pierre, *Chemistry – A European Journal*, 2006, **12**, 6953-6962.
28. T. Singh Lobana, P. Kumari, R. Sharma, A. Castineiras, R. J. Butcher, T. Akitsu and Y. Aritake, *Dalton Transactions*, 2011, **40**, 3219-3228.
29. P. K. Suganthy, R. N. Prabhu and V. S. Sridevi, *Tetrahedron Letters*, 2013, **54**, 5695-5698.
30. A. M. Pyle, J. P. Rehmann, R. Meshoyrer, C. V. Kumar, N. J. Turro and J. K. Barton, *Journal of the American Chemical Society*, 1989, **111**, 3051-3058.
31. X.-L. Wang, H. Chao, H. Li, X.-L. Hong, Y.-J. Liu, L.-F. Tan and L.-N. Ji, *Journal of Inorganic Biochemistry*, 2004, **98**, 1143-1150.
32. H. Chao, W.-J. Mei, Q.-W. Huang and L.-N. Ji, *Journal of Inorganic Biochemistry*, 2002, **92**, 165-170.
33. P. Krishnamoorthy, P. Sathyadevi, A. H. Cowley, R. R. Butorac and N. Dharmaraj, *European Journal of Medicinal Chemistry*, 2011, **46**, 3376-3387.
34. J.Prousek, *Pure and Applied Chemistry*, 2007, **79**, 2325-2338.
35. H. Liu, L. Li, Q. Guo, J. Dong and J. Li, *Transition Metal Chemistry*, 2013, **38**, 441-448.
36. V. Uma, M. Kanthimathi, T. Weyhermuller and B. U. Nair, *Journal of Inorganic Biochemistry*, 2005, **99**, 2299-2307.
37. S. Satyanarayana, J. C. Dabrowiak and J. B. Chaires, *Biochemistry*, 1993, **32**, 2573-2584.
38. S. Satyanarayana, J. C. Dabrowiak and J. B. Chaires, *Biochemistry*, 1992, **31**, 9319-9324.
39. C. V. Kumar and E. H. Asuncion, *Journal of the American Chemical Society*, 1993, **115**, 8547-8553.
40. L. Messori, P. Orioli, D. Vullo, E. Alessio and E. Iengo, *European Journal of Biochemistry*, 2000, **267**, 1206-1213.
41. Y. Wang, X. Wang, J. Wang, Y. Zhao, W. He and Z. Guo, *Inorganic Chemistry*, 2011, **50**, 12661-12668.
42. S.-J. Lau and B. Sarkar, *Journal of Biological Chemistry*, 1971, **246**, 5938-5943.
43. D. Senthil Raja, G. Paramaguru, N. S. P. Bhuvanesh, J. H. Reibenspies, R. Renganathan and K. Natarajan, *Dalton Transactions*, 2011, **40**, 4548-4559.
44. D. Senthil Raja, N. S. P. Bhuvanesh and K. Natarajan, *European Journal of Medicinal Chemistry*, 2011, **46**, 4584-4594.
45. M. Lee, A. L. Rhodes, M. D. Wyatt, S. Forrow and J. A. Hartley, *Biochemistry*, 1993, **32**, 4237-4245.
46. J.R.Lakowicz, *Fluorescence Quenching: Theory and applications. Principles of Fluorescence spectrscopy*, Kluwer Academic/plenum Publishers, New York, 1999.
47. X.-Z. Feng, Z. Lin, L.-J. Yang, C. Wang and C.-l. Bai, *Talanta*, 1998, **47**, 1223-1229.
48. Y.-J. Hu, Y. Ou-Yang, C.-M. Dai, Y. Liu and X.-H. Xiao, *Biomacromolecules*, 2009, **11**, 106-112.
49. X. Z. H. G.Z.Zen, J.G.Xu,Z.Z.Zheng and Z.B.Wang, *Methods of Fluorescence Analysis*, Science press, Beiging, 2 edn., 1990.
50. C. W. Fuller and J. N. Miller, *Proceedings of the Analytical Division of the Chemical Society*, 1979, **16**, 199-208.
51. H. Xu, N. Yao, H. Xu, T. Wang, G. Li and Z. Li, *International Journal of Molecular Sciences*, 2013, **14**, 14185-14203.
52. M. Milenković, A. Bacchi, G. Cantoni, J. Vilipić, D. Sladić, M. Vujčić, N. Gligorijević, K. Jovanović, S. Radulović and K. Anđelković, *European Journal of Medicinal Chemistry*, 2013, **68**, 111-120.
53. P. Sathyadevi, P. Krishnamoorthy, R. R. Butorac, A. H. Cowley, N. S. P. Bhuvanesh and N. Dharmaraj, *Dalton Transactions*, 2011, **40**, 9690-9702.
54. Marco H. Klingele and S. Brooker, *European Journal of Organic Chemistry*, 2004, **2004**, 3422-3434.
55. R. Manikandan, P. Anitha, G. Prakash, P. Vijayan and P. Viswanathamurthi, *Polyhedron*, 2014, **81**, 619-627.
56. SADABS: Area- Detector Absorption Correction; Siemens Industrial Automation, WI,1996.
57. A. Altomare, G. Cascarano, C. Giacovazzo and A. Guagliardi, *Journal of Applied Crystallography*, 1993, **26**, 343-350.
58. G. Sheldrick, *Acta Crystallographica Section A*, 2008, **64**, 112-122.
59. Bruker-Nonious(2004) and M. Bruker Axs Inc., Wisconsin, USA.
60. J. Bernadou, G. Pratviel, F. Bennis, M. Girardet and B. Meunier, *Biochemistry*, 1989, **28**, 7268-7275.
61. P. Lincoln, E. Tuite and B. Nordén, *Journal of the American Chemical Society*, 1997, **119**, 1454-1455.
62. B. Nordén and F. Tjerneld, *Biopolymers*, 1982, **21**, 1713-1734.
63. J. B. Chaires, N. Dattagupta and D. M. Crothers, *Biochemistry*, 1982, **21**, 3933-3940.
64. G. Cohen and H. Eisenberg, *Biopolymers*, 1969, **8**, 45-55.
65. M. S. Blois, *Nature*, 1958, **181**, 1199-1200.
66. T. Nash, *Biochemical Journal*, 1953, **55**, 416-421.
67. L. C. Green, D. A. Wagner, J. Glogowski, P. L. Skipper, J. S. Wishnok and S. R. Tannenbaum, *Analytical Biochemistry*, 1982, **126**, 131-138.
68. T. Mosmann, *Journal of Immunological Methods*, 1983, **65**, 55-63.